

# ELECTRICAL CHARACTERIZATION OF MAGNETORESISTIVE SENSORS BASED ON AMR AND GMR EFFECTS USED FOR LAB-ON-A-CHIP APPLICATIONS

Marius Volmer<sup>1</sup> and Marioara Avram<sup>2</sup>

<sup>1</sup>Physics Department, Transilvania University, 29 Eroilor, Brasov 500036, Romania

<sup>2</sup>National Institute for Research and Development in Microtechnologies, Str. Erou Iancu Nicolae 32B, 72996 Bucharest, Romania

Received: January 22, 2007

**Abstract.** Angular dependencies are investigated for the planar Hall effect (PHE) in Permalloy ( $\text{Ni}_{80}\text{Fe}_{20}$ ) thin films and Permalloy based multilayered structures used as rotation sensors in lab-on-a-chip applications. A distortion of the angular dependence symmetry with respect to the abscissa axis was observed. This is due to contacts misalignment, hysteresis behaviour of the magnetic material and some coupling effects in the multilayered structure. We performed micromagnetic simulations to discuss the effect of the magnetic field strength on the shape of the angular dependence of PHE. From experimental measurements and micromagnetic simulations, made on the multilayered structure, results a distortion of the angular dependence of the PHE for magnetic fields less than 16 kA/m (200 Oe) because the magnetization vector can not follow the direction of the applied magnetic field. Using a special setup in which we made PHE measurements over two orthogonal directions will give a rotation sensor with an improved symmetry of the output signal and an angular resolution bellow  $0.5^\circ$ .

## 1. INTRODUCTION

The magnetoresistive sensors made from Permalloy thin films and Permalloy based multilayered structures are very attractive for detection of low magnetic fields and as rotation sensors. The resistance behaviour of Permalloy based thin films (3d ferromagnetic alloys) is anisotropic with respect to the applied field direction, the MR being positive when the magnetic field is parallel to the current (longitudinal) and negative when the magnetic field is perpendicular to the current direction (transversal). This is the anisotropic magnetoresistance effect (AMR). It is important to mention that the MR effect in ferromagnetic thin films is determined by the sample magnetization rather than the external

magnetic field. In other words, galvanomagnetic effects like MR and Hall effect are strongly related with the magnetic properties of these structures. Because of the AMR effect will appear an electric field perpendicular to the applied current even when the magnetic field is in the film plane. This is the planar Hall effect (PHE). Using a Hall effect geometry we get direct access to the anisotropic part of the resistance with the advantage of a reduced thermal drift of the output signal. In a single domain approximation, the PHE voltage is determined by the relation [1]:

$$U = C \cdot M^2 j \sin 2\theta, \quad (1)$$

where  $C$  is a constant determined by the material properties,  $j$  is the current density,  $M$  is the saturation

---

Corresponding author: Marius Volmer, e-mail: volmerm@unitbv.ro

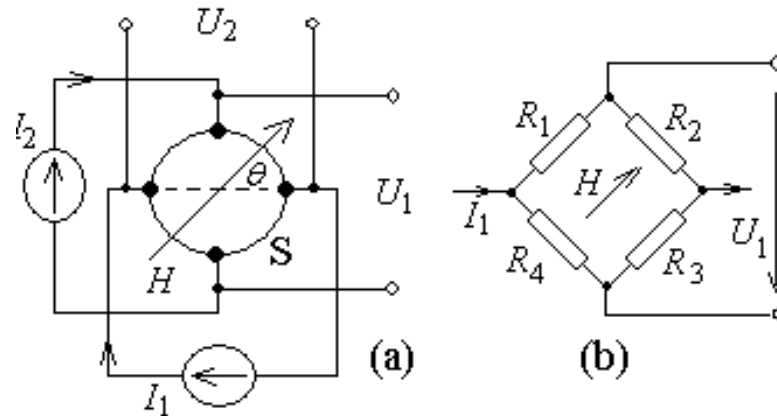


**Fig. 1.** (a) Schematic setup used for PHE measurements and (b) the four-resistor arrangement model to account for the electric behaviour of the sample.  $H$  is applied in the sample plane.

tion magnetization and  $\theta$  is the angle between the current and the magnetization vector that, in turn, is determined by the value and direction of the external magnetic field. From Eq. (1) we see that the PHE effect can provide information about the magnetic properties of the material and, because of the angular dependence  $\sim \sin 2\theta$ , allows building of rotation sensors. In this work we present results regarding the angular dependence of the PHE for three samples: (i) a  $\text{Ni}_{80}\text{Fe}_{20}$  (10 nm) thin film, (ii) a  $\text{Ni}_{80}\text{Fe}_{20}$  (10 nm)/Cu (4 nm)/ $\text{Ni}_{80}\text{Fe}_{20}$  (10 nm) multilayer structure (ML) and (iii) a  $\text{Ni}_{80}\text{Fe}_{20}$  (2 nm)/ $\text{Al}_2\text{O}_3$  (1 nm)/ $\text{Ni}_{80}\text{Fe}_{20}$  (2 nm) nanogranular film. The measurements were made both in dc and ac currents.

We observed some strong distortions of the angular dependence of the PHE voltage at low magnetic fields in the case of the ML structure. This is because the PHE voltage depends on the angle between the current and magnetization vector and, at low magnetic fields, the magnetization vector cannot follow accurately the direction of the applied magnetic field. We confirmed this behaviour by micromagnetic simulations.

## 2. EXPERIMENTAL

The samples were grown on oxidised Si(100) substrates by thermal deposition from  $\text{Al}_2\text{O}_3$  crucibles. The sample (ii) contains a single trilayer structure. The substrate was positioned over the desired source, Py or Cu, using a rotating platform. This setup allows in-situ deposition of the ML structure.

In what follows we give some details regarding the deposition of the Py(2 nm)/ $\text{Al}_2\text{O}_3$ (1 nm)/Py(2 nm) structure. First was deposited, on the oxidised Si substrate, the Py(2 nm) layer and then the Al(1 nm) layer. The  $\text{Al}_2\text{O}_3$  insulating layer was formed by oxidation of the Al layer in air at 260 Pa and 50 °C for 60 minutes. Because the 2 nm Py layer is slight above the percolation limit [2] its surface is very rough. The rms surface roughness is about 1.5 nm which is more than the thickness of the  $\text{Al}_2\text{O}_3$  insulating layer. Finally we deposited on to  $\text{Al}_2\text{O}_3$  the second (top) layer of Py(2 nm). In this way we obtained a structure which is most likely a mixture between Py and  $\text{Al}_2\text{O}_3$  layers. The deposition mask has circular shape with 5 mm in diameter. The four-lead setup and the equivalent resistor arrangement model [3] are presented in Fig. 1. The connections consist in 4 Cu strips placed on the corners of a square of 4 mm each side, like in Fig. 1a. The Cu strips were deposited in-situ, i.e. prior to introduce the air in the deposition chamber, by using a second deposition mask. The dc current sources  $I_1$  and  $I_2$  drive the same current  $V, I$ , through the sample, S, and are computer controlled. When the source  $I_1$  is on, the source  $I_2$  is off, the measured voltage is  $U_1$ . When the source  $I_2$  is on, the source  $I_1$  is off, the measured voltage is  $U_2$ . In this way, for a given angle,  $\theta$ , between the magnetic field,  $H$ , and the direction of the current driven by  $I_1$ , we made two measurements for the PHE. Because for an ideal experimental setup  $U_1=U_2$  we will take as reference for angle measurements the direction of the current  $I_1$  for both measurements. This

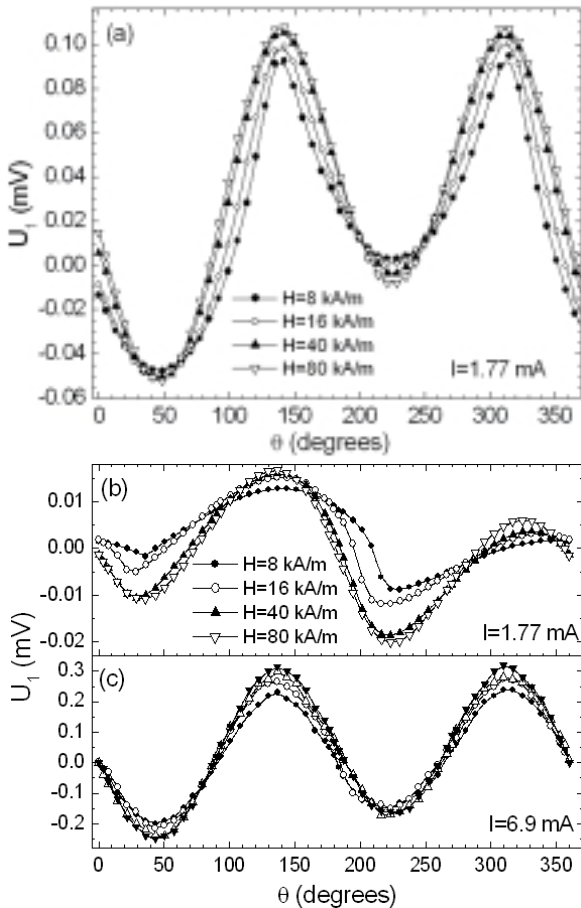


**Fig. 2.** Angular dependence of the PHE effect, for different values of the applied field, measured for (a)  $\text{Ni}_{80}\text{Fe}_{20}$  (10 nm) film, (b)  $\text{Ni}_{80}\text{Fe}_{20}$  (10 nm)/Cu(4 nm)/ $\text{Ni}_{80}\text{Fe}_{20}$  (10 nm) ML and (c)  $\text{Ni}_{80}\text{Fe}_{20}$  (2 nm)/ $\text{Al}_2\text{O}_3$  (1 nm)/ $\text{Ni}_{80}\text{Fe}_{20}$  (2 nm) nanogranular film.

is because in equation 1,  $\sin 2\theta$  becomes  $\sin[2(\pi/2-\theta)]$ , see Figs. 1a and 1b. The measurement system is composed from a two channel instrumentation amplifier, a LabJack DAQ card and a NI 4351, 24 bit, DAQ card for high resolution readings. When  $\theta=0$ , the PHE voltage has a minimum value because the MR effect will have the same amplitude and sign for all the resistors from the equivalent Wheatstone bridge. However, the measured PHE voltage is not zero, for  $\theta=0$ , because of the residual offset (misalignment of the contacts) and because the magnetization is not following accurately the direction of the magnetic field. When  $\theta=45^\circ$ , like in Fig. 1, the resistors  $R_{1,3}$  will experience a positive MR effect (longitudinal MR) whereas the resistors

$R_{2,4}$  will experience a negative MR effect (transversal MR) and the PHE will have a maximum value. This measurement setup gets the maximum response from the AMR effect. To obtain the frequency dependence of the PHE voltage, we used the same experimental configuration presented in Fig. 1 in which the source  $I_1$  is driven by a Bode analyser, through a voltage  $U_0$ , and takes frequencies from 20 Hz to 35 kHz. The output signal  $U_1$  is buffered by the instrumentation amplifier and applied also to the Bode analyzer which returns a value  $R=20\cdot\log(A\cdot U_1/U_0)$ , in dB, that is proportional with the PHE voltage.  $A$  is the gain of the instrumentation amplifier.

### 3. RESULTS AND DISCUSSION

Fig. 2 presents the angular dependence of the PHE effect, voltage  $U_1$ , for the investigated samples. This means that the source  $I_1$  is ON and the source  $I_2$  is OFF. The angle  $\theta$  between the applied magnetic field and the direction of the current  $I_1$  is illustrated in Fig. 1a. Because of the contacts misalignments the angular behaviour of the PHE, voltage  $U_1$ , is distorted. We see that for the ML sample, Fig. 2b, the angular dependencies of the PHE voltage for low magnetic fields ( $H=8$  and  $16$  kA/m respectively) present some irregularities and are far from the shape predicted by the Eq. (1). This is because the magnetization cannot follow accurately the direction of the magnetic field due to the coupling between the magnetic layers through the Cu layer. To understand this behaviour we present, in Fig. 3a, the results of the micromagnetic simulation regarding the angular dependence of the ML magnetization for different values ( $H=8, 16$  and  $40$  kA/m) of the rotating magnetic field. To run these simulations we used complex structures of single domains of Permalloy which interact between them and with the applied magnetic field [4]. As we can see from Fig. 3a, the magnetization of the ML structure follows the direction of the magnetic field when  $H=40$  kA/m (500 Oe). Fig. 3b presents a picture of the magnetic moments orientation, in the ML structure, taken during the micromagnetic simulation when the rotating applied field was  $8$  kA/m and  $\theta=45^\circ$ . The field starts to rotate from  $\theta=0$  and makes a complete rotation. This picture, Fig. 3b, illustrates the fact that the magnetic moments cannot follow the direction of the applied magnetic field. The angular dependencies, Fig. 2b, of the PHE are almost the same for  $H=40$  and  $80$  kA/m respectively. The small differences between the curves for the NiFe(10 nm) film, Fig. 2a, show us that the sample

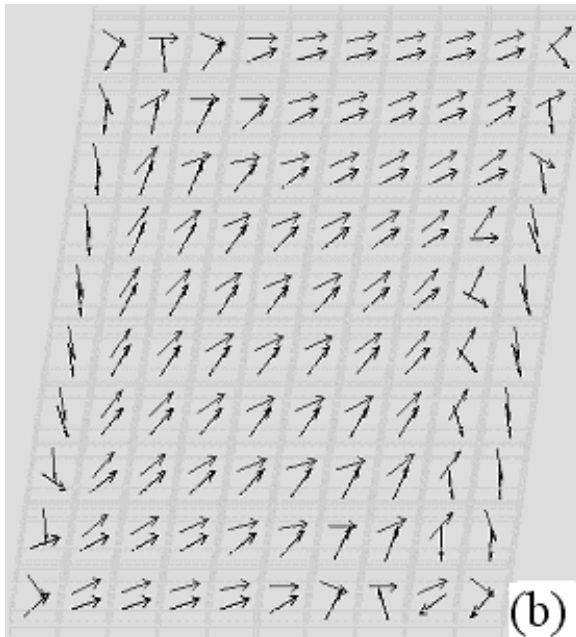
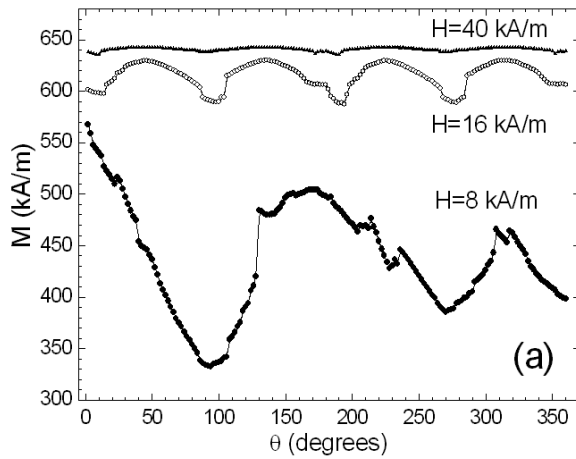


**Fig. 3.** (a) A micromagnetic simulation of the angular dependence of the magnetization for the  $\text{Ni}_{80}\text{Fe}_{20}$ (10 nm)/Cu(4 nm)/ $\text{Ni}_{80}\text{Fe}_{20}$ (10 nm) ML structure and (b) the micromagnetic simulation regarding the orientation of magnetic moments when the applied magnetic field,  $H=8$  kA/m, makes  $45^\circ$  with the direction of the current  $I_x$ .

saturates, easily, for fields higher than 8 kA/m and the magnetization follow the direction of the magnetic field.

The frequency dependence of the PHE voltage was measured, using a Bode analyzer, for different orientations of the samples in magnetic field. The results are presented in Fig. 4. The positions of the curves for different angles, relative to zero level, are correlated with the measured PHE voltages as presented in Fig. 2 but don't reflect the

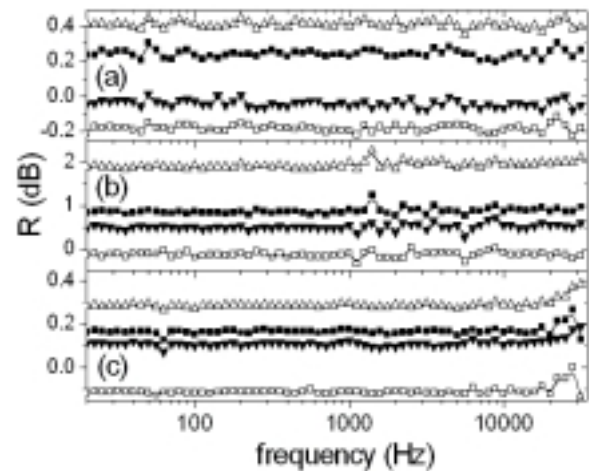


**Fig. 4.** The frequency dependence of the PHE voltage measured for (a)  $\text{Ni}_{80}\text{Fe}_{20}$ (2 nm)/ $\text{Al}_2\text{O}_3$ (1 nm)/ $\text{Ni}_{80}\text{Fe}_{20}$ (2 nm) nanogranular film, (b)  $\text{Ni}_{80}\text{Fe}_{20}$ (10 nm)/Cu(4 nm)/ $\text{Ni}_{80}\text{Fe}_{20}$ (10 nm) ML structure and (c)  $\text{Ni}_{80}\text{Fe}_{20}$ (10 nm) thin film for different orientations of the samples in magnetic field ( $\square$ -  $45^\circ$ ,  $\blacksquare$ -  $90^\circ$ ,  $\triangle$ -  $135^\circ$ ,  $\blacktriangledown$ -  $180^\circ$ ).

real amplitude of the PHE that appears in the samples. The frequency response is almost flat for the nanogranular, Fig. 4a, and multilayer, Fig. 4b, structures. The high resistivity and the small magnetic fraction in the nanogranular structure can be some reasons for this behaviour. The nonmagnetic layer of Cu(4 nm) lowers the magnetic permeability of the structure and plays a shunting effect for the ac current. It is not very clear what is the reason of the small increasing of the PHE voltage at high frequency for the Permalloy layer, as we see in Fig. 4c. If we look at the equivalent model, presented in Fig. 1b, the resistors have to be replaced, at high frequency, with a more complex structure which presents in addition inductances. The unbalance of the bridge with reactive components which present inductances, can be higher, under the action of a magnetic field, than in the case when the bridge consists only from resistor. For high frequencies the capacitive effects decrease the output voltage of the bridge.

Despite of the good response of the  $\text{Ni}_{80}\text{Fe}_{20}$ (2 nm)/ $\text{Al}_2\text{O}_3$ /  $\text{Ni}_{80}\text{Fe}_{20}$ (2 nm) nanogranular film, the thermal stability is not good because of the conduction mechanism through the oxide barriers which give us a negative thermal coefficient of the resistivity.

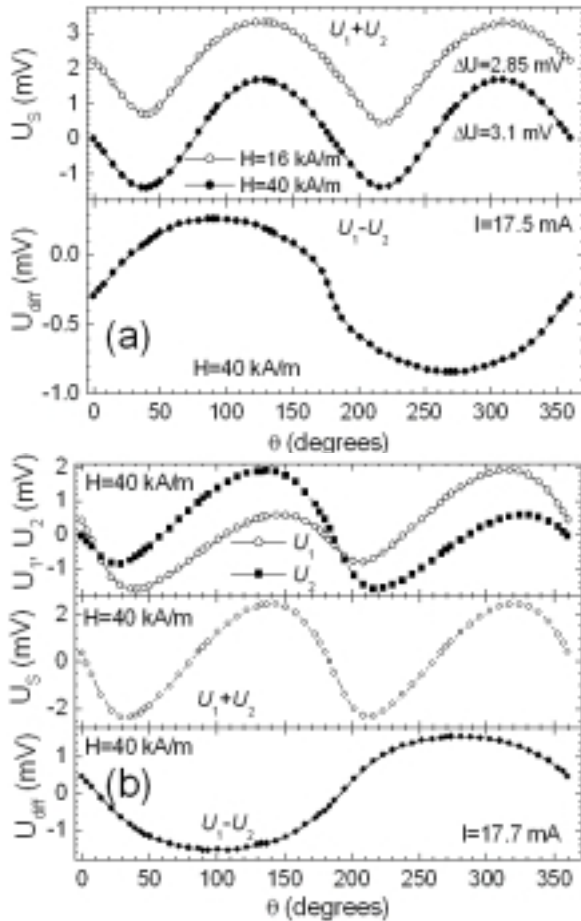


**Fig. 5.** The results of the angular dependence of the PHE measurements made over two orthogonal directions for (a)  $\text{Ni}_{80}\text{Fe}_{20}$  (10 nm) thin film and (b)  $\text{Ni}_{80}\text{Fe}_{20}$  (10 nm)/Cu(4 nm)/ $\text{Ni}_{80}\text{Fe}_{20}$  (10 nm) multilayer structure.

To compensate the errors due to contacts misalignment and to increase the sensor sensitivity we made two measurements of the PHE for each angle over two orthogonal directions using the setup presented in Fig. 1a. Other authors use two orthogonal PHE sensors [5] and perform the same kind of measurements in order to improve the angular resolution. Making the PHE measurements for Permalloy and the ML structure over these two orthogonal directions we obtained, by summing the voltages  $U_1$  and  $U_2$ , a response of the sensor which is well described by the Eq. (1). The results of these measurements made on  $\text{Ni}_{80}\text{Fe}_{20}$  (10 nm) and  $\text{Ni}_{80}\text{Fe}_{20}$  (10 nm)/Cu(4 nm)/ $\text{Ni}_{80}\text{Fe}_{20}$  (10 nm) thin films, are presented in Fig. 5. The calculated val-

ues  $U_S = U_1 + U_2$  give us the output of the microcompass sensor with a sinusoidal behaviour with two periods for a complete rotation. To explain the behaviour of the difference voltage,  $U_{\text{diff}} = U_1 - U_2$ , which give us a single period sinusoid for a complete rotation we have to look at dependencies  $U_1$  and  $U_2$  from the Fig. 5b. We believe that this voltage arises from the contacts misalignment errors.

## 4. CONCLUSIONS

We studied the angular response of the PHE for three systems: (i)  $\text{Ni}_{80}\text{Fe}_{20}$  (10 nm) film, (ii)  $\text{Ni}_{80}\text{Fe}_{20}$  (10 nm)/Cu(4 nm)/ $\text{Ni}_{80}\text{Fe}_{20}$  (10 nm) multilayer structure and (iii)  $\text{Ni}_{80}\text{Fe}_{20}$  (2 nm)/ $\text{Al}_2\text{O}_3$  (1 nm)/ $\text{Ni}_{80}\text{Fe}_{20}$  (2 nm) nanogranular film and by micromagnetic simulations we show the origin of the distortions which can be seen for low magnetic fields. By making PHE measurements over two orthogonal directions for each angle, we were able to compensate the errors that appear due to contact misalignments, hysteresis effects and homogeneities defects. From the above measurements and micromagnetic simulations the optimum value of the magnetic field strength is 40 kA/m. For this value, the response of the sensor made from Permalloy follows very well a sinusoidal shape, Fig. 5a, with two periods for a complete rotation and a sensitivity of about 33 mV/°, when  $\theta$  varies from 45° to 135°. For the ML sample, the sensitivity is about 46 mV/° for the same variation of the angle  $\theta$ , Fig. 5b. The angular resolution is, in both cases, below 0.5° and depends on the driving current through the sensor, on the precision of assembling and the thermal stability of the equivalent Wheatstone bridge. This method can be used to obtain low cost rotation sensors for microcompass applications.

## REFERENCES

- [1] E.M. Epshtein, A.I. Krikunov and Yu.F. Ogrin // *J. Magn. Magn. Mater.* **258-259** (2003) 80.
- [2] T. Lucinski, G. Reis, N. Matern and L.van Luyen // *J. Magn. Magn. Mater.* **189** (1999) 39.
- [3] C. Prados, D. Garcia, F. Lesmes, J. J. Freijo and A. Hernando // *Appl. Phys. Lett.* **67** (1995) 718.
- [4] M. Volmer and J. Neamtu // *Physica B* **372** (2006) 198.
- [5] F. Montaigne, A. Schuhl, F. Nguyen Van Dau and A. Encinas // *Sensors and Actuators* **81** (2000) 324.